Electronic Supplementary Material (ESI) for Chemical Communications
This journal is © The Royal Society of Chemistry 2013

[Supporting Information (SI) to accompany:]

A facile synthesis of UiO-66, UiO-67 and their derivatives

Michael J. Katz,[a,†] Zachary J. Brown,[a,†] Yamil J. Colón,[b] Paul W. Siu,[a] Karl A. Scheidt,[a] Randall Q. Snurr,[b] Joseph T. Hupp[a,*] and Omar K. Farha[a,*]

[a]*Department of Chemistry and International Institute for Nanotechnology, Northwestern University, 2145 Sheridan Road, Evanston, Illinois 60208-3113,*
[b] *Department of Chemical & Biological Engineering, Northwestern University, 2145 Sheridan Road, Evanston, Illinois 60208-3120*

[†] *Authors contributed equally.*

Table of Contents

Section S1. General procedures, materials, and instrumentations.

2-hydroxyterephthalic acid, 2-nitrobiphenyl-4,4'-dicarboxylic acid and 2-amino-4,4'-dicarboxylic acid were synthesized as described previously.[1-3] All other reagents were used as received. Terephthalic acid (BDC), $ZrCl_4$, 2-nitroterephthalic acid, 2,5-diaminoterephthalic acid, 2,5-diohydroxyterephthalic acid, and 4,4'-biphenyldicarboxylic acid (BPDC) were purchased from Sigma-Aldrich. *N*,*N*'-dimethylformamide and reagent alcohol were purchased from Macron Chemicals. 2-aminoterephthalic acid was purchased from Alfa Aesar.

Powder X-ray diffraction (PXRD) patterns were obtained using a Rigaku X-ray Diffractometer Model ATX-G (Tokyo, Japan) equipped with an 18 kW Cu rotating anode, MLO

This journal is © The Royal Society of Chemistry 2013

monochromator, and a high-count rate scintillation detector. Measurements were made over a range of $2° < 2\theta < 40°$ in 0.05 step size at a scanning rate of 1 deg/min.

TGA experiments were performed on a Mettler Toledo TGA/DSC 1 Star^e System (Schwerzenbach, Switzerland) interfaced with a PC using Star^e software (version 9.10). Samples were placed in alumina pans and heated at a rate of 7 °C/min from 25-800°C under a nitrogen atmosphere.

Diffuse reflectance infrared spectra (DRIFTS) were recorded on a Nicolet 7600 FTIR spectrometer equipped with an MCT detector cooled to 77 K. The spectra were collected in a KBr mixture under N_2 purge (samples prepared in atmosphere). Pure KBr was measured as the background and subtracted from sample spectra.

Supercritical CO_2 drying was performed using a Tousimis^{TM} Samdri® PVT-30 critical point dryer (Tousimis, Rockville, MD, USA). Supercritically dried samples were prepared in the following manner. The solvent from freshly prepared samples was decanted and replaced with DMF solvent. The product was allowed to settle over the course of 2 hours. This process was repeated 2x with DMF followed by 3x with ethanol. The ethanol-dispersed sample was transferred into a Tousimis Samdri-PVT-3D supercritical CO_2 dryer. The temperature was lowered to 0 °C, and the chamber was filled with liquid CO_2 (ultrahigh grade CO_2 with a siphon from Air-Gas Inc was used). The sample was soaked for 8 hours total, venting for five minutes every two hours. The chamber was then heated to 40 °C, and the supercritical CO_2 was bled off at a rate of 1 mL/min until the chamber reached ambient pressure (approximately 12 hours). The chamber was opened and the sample was quickly sealed and taken into an argon atmosphere glove box for further manipulations. The dried sample was transferred into a pre-weighed glass sample tube which was sealed and quickly transferred to a system providing 10^{-4} torr dynamic vacuum. The sample was kept under vacuum at room temperature for 6 hours and was then used for N_2 adsorption measurements. After measurement the sample was returned to the argon atmosphere glove box and a final mass was calculated.

N_2 adsorption and desorption isotherm measurements were performed on a Micromeritics Tristar II 3020 (Micromeritics, Norcross, GA) at 77K. Before each isotherm, samples were activated either via supercritical CO_2 drying or by heating for 3 hours under high vacuum on an ASAP-2020 (Micromeritics, Norcross, GA). The temperature used for each sample is listed in Table S1. Between 30 and 100 mg of material was used for each measurement. Data was analyzed using the ASAP 2020 software (Micromeritics, Norcross, GA). All gases used were Ultra High Purity Grade 5 as obtained from Airgas Specialty Gases (Chicago, IL).

This journal is © The Royal Society of Chemistry 2013

Section S2. Synthesis of UiO-66 and -67 materials

All UiO materials were synthesized using the following general procedure and the amounts of reagents listed in Table S1. An 8-dram vial was loaded with $ZrCl_4$, one third of the DMF, and concentrated HCl before being sonicated for 20 minutes until fully dissolved. The ligand and the remainder of the DMF were then added and the mixture was sonicated an additional 20 minutes before being heated at 80 °C overnight (BPDC was not completely soluble under these conditions). The resulting solid was then filtered over a fine frit and washed first with DMF (2x 30 mL) and then with EtOH (2x 30 mL). The sample was filtered for several hours to remove all residual solvent. With the exception of the supercritically dried samples, the samples were activated by first heating to 90 °C under vacuum until a pressure of 100 mtorr was reached. The samples were then subjected to the temperatures listed in Table S1 for 3 hours prior to measuring N_2 isotherms. UiO-67 isotherms and PXRDs are shown in Figures S1 and S2, respectively.

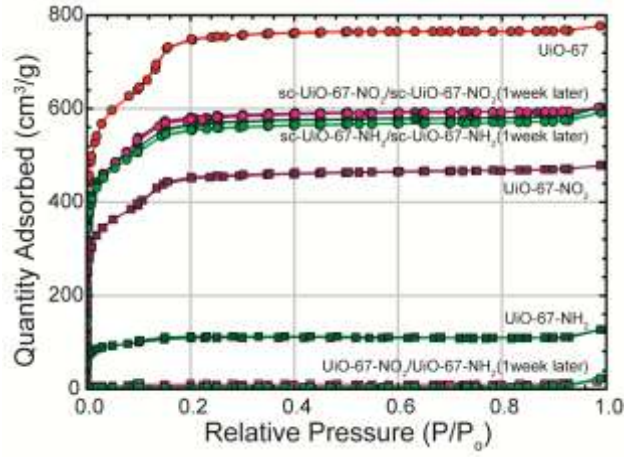

Figure S1. Isotherms of UiO-67 and derivatives activated via heating at 100 °C and supercritical CO_2 drying (labeled sc).

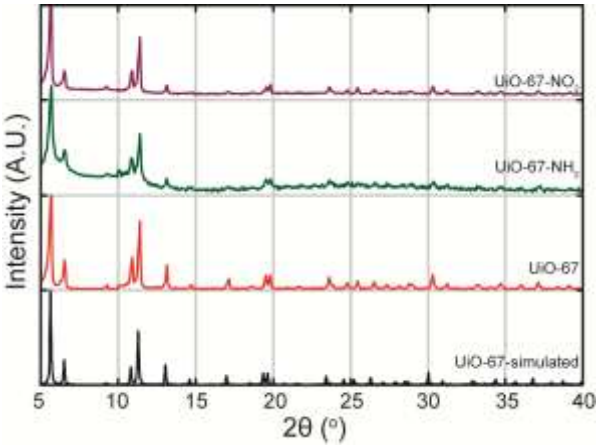

Figure S2. PXRDs of UiO-67 derivatives synthesized in this work.

This journal is © The Royal Society of Chemistry 2013

Table S1. Experimental parameters for the synthesis of UiO derivatives described in this work. Supercritical CO_2 drying is denoted sc-CO_2.

	Mass ligand (mg)	Mass $ZrCl_4$ (mg)	Volume HCl (mL)	Volume DMF (mL)	Vial Size (dram)	Activation Temperature (°C)
UiO-66	123 (0.75 mmol)	125 (0.54 mmol)	1	15	8	150
UiO-66-NH_2	134 (0.75 mmol)	125 (0.54 mmol)	1	15	8	150
UiO-66-OH	135 (0.75 mmol)	125 (0.54 mmol)	1	15	8	150
UiO-66-NO_2	158 (0.75 mmol)	125 (0.54 mmol)	1	15	8	150
UiO-66-$(NH_2)_2$	146 (0.75 mmol)	125 (0.54 mmol)	1	15	8	100
UiO-66-$(OH)_2$	147 (0.75 mmol)	125 (0.54 mmol)	1	15	8	100
UiO-67	90 (0.38 mmol)	67 (0.27 mmol)	0.5	15	8	150
UiO-67-NH_2	92 (0.38 mmol)	67 (0.27 mmol)	0.5	15	8	sc-CO_2
UiO-67-NO_2	103 (0.38 mmol)	67 (0.27 mmol)	0.5	15	8	sc-CO_2

Section S3. Influence of HCl concentration on UiO synthesis and surface area.

The figures below illustrate the rate of observation of MOF as a function of time and HCl concentration. From left to right, the amount of HCl used decreases from 1.0 to 0.5 to 0.25 to 0.1 mL. It is clear that as the concentration of HCl decreases, the rate of observation of UiO-66 decreases. SEM analysis of the UiO-66 made in this manner show that when the volume of HCl is 0.25 mL or greater, the particle size remains unchanged. Surface area measurements of these materials demonstrate that the higher HCl concentration leads to larger surface areas.

This journal is © The Royal Society of Chemistry 2013

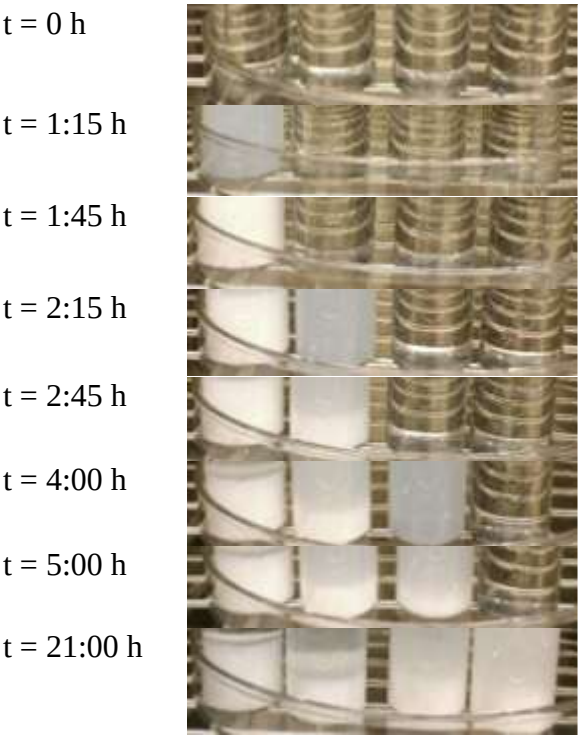

Figure S3. Time lapse photos of UiO-66 made with various amounds of HCl. From left to right: 1.0 mL, 0.5 mL, 0.25 mL, 0.10 mL.

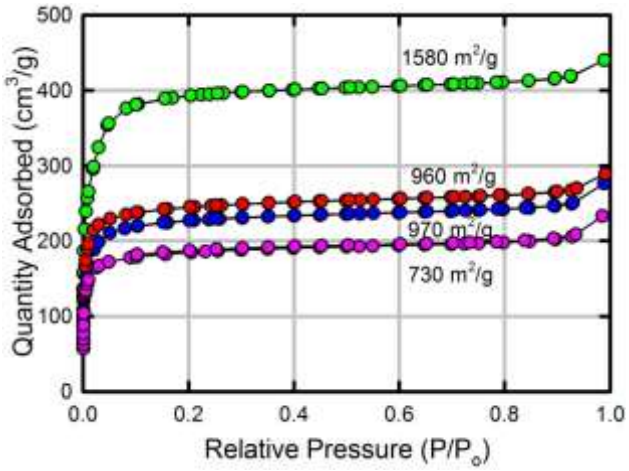

Figure S4. Isotherms of UiO-66 made with 1 mL (green), 0.5 mL (Red), 0.25 mL (Blue) and 0.1 mL (purple) of HCl.

Section S4. Comparison of UiO-66 made with HCl and acetic acid.

Elemental analysis of UiO-66 made with HCl or with acetic acid is shown in Table S2. The elemental analysis is consistent with the observation that the HCl synthesized UiO-66 has 2 linkers missing per formula unit. It should be noted, that while the addition of DMF and

This journal is © The Royal Society of Chemistry 2013

ethanol/water is necessary to achieve agreement between observed and calculated elemental composition, the possibilities for incorporated guests are numerous and thus too complex to accurately assess – hence, the calculated and observed vary more than usual. However, the higher Zr and lower C content in the HCl-synthesized UiO-66 is consistent with a decrease in the amount of linkers.

Table S2. Elemental Analysis of UiO-66 made with HCl, and with acetic acid as the modulator.

Complex	% C	% H	% N	% Cl	% Zr
Observed HCl synthesis	31.18	2.71	1.96	0.98	31.91
Calculated for $Zr_6O_4(OH)_4(BDC)_4(Cl)_{0.4}(OH)_{3.6}(DMF)_2$ $(EtOH)_{2.5}$	30.88	3.16	1.67	0.84	32.72
Observed Acetic acid synthesis	35.18	2.76	2.03	0.0	30.16
Calculated for $Zr_6O_4(OH)_4(BDC)_6(DMF)_2(H_2O)_2$	35.12	2.51	1.51	0.0	29.64

[a] Elemental analysis of MOFs can vary depending of the trace amount of solvent that remain in the pores.

Pore size distribution of UiO-66 illustrates that when all the linkers are present, there is a well-defined pore at ca. 8.5 Å. However, when HCl is used, and about 4 linkers per node are missing, then this pore shifts to ca. 11.5 Å. This is consistent with missing linkers increasing the average size of the small tetrahedral pore in UiO-66.

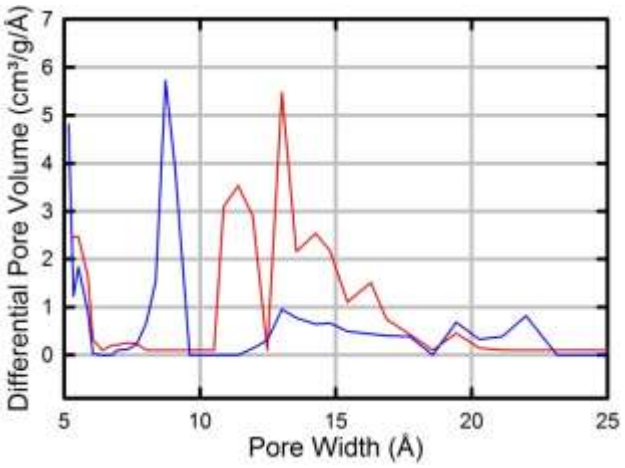

Figure S5. Pore-size distribution for UiO-66 with a full complement of ligands[4] (blue), and with only 8 linkers per node (red).

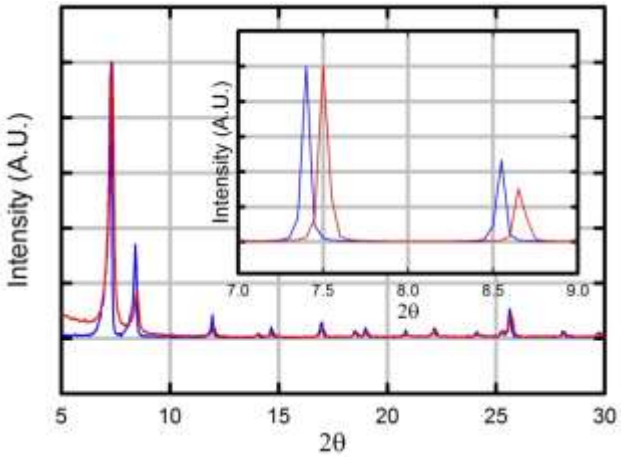

Figure S6. Observed and Simulated (inset) of HCl-synthesized (red) and conventional (acetic acid modulated) UiO-66.

Simulated PXRD patterns were obtained using the Reflex tools integrated in Matierials Studio.[5] Figure S6 reports the experimental and simulated PXRD patterns obtained for modulated UiO-66[4] and UiO-66 synthesized with our HCl protocol. The fact that the UiO-66 synthesized using HCl has fewer linkers should be reflected in the intensity of the peaks of the PXRD. In particular, the second reflection, the *200*, in the PXRD for the structures with missing linkers decreases in intensity in both the experimental and simulated patterns.

Section S5. Influence of DMF purity/additives on UiO synthesis

Nitrogen isotherms were collected for 4 different UiO-66-NH_2 samples to ensure that HCl was the primary factor in the reproducible synthesis of UiO-66-NH_2. When the only synthesis solvent is DMF, then the surface area is 830 m^2/g; this is similar to the majority of literature values of UiO-66-NH_2.[6-8] However, as demonstrated in Figure S3, the surface area is optimized when 1 mL of concentrated HCl is added to the DMF solution as described above (1200 m^2/g). Our concern was that the HCl was merely a spectator, and the water in the HCl solution is crucial.[4] Samples prepared with the addition of 1 mL of H_2O in 15 mL of DMF showed the lowest surface area for UiO-66-NH_2 (360 m^2/g). Additionally, it should be noted that when the DMF is purified by column chromatography to remove any residual water and dimethylamine, the decomposition product of DMF, then the surface area is also compromised (660 m^2/g).

This journal is © The Royal Society of Chemistry 2013

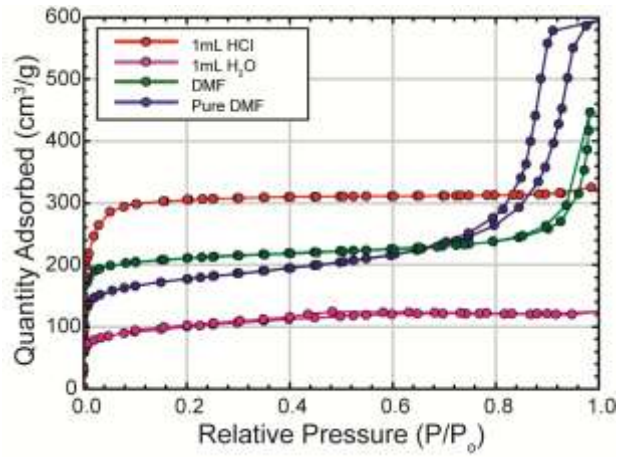

Figure S7. N_2 Isotherms of UiO-66-NH_2 samples synthesized using varying qualities of DMF.

Section S6. Thermal gravitational analysis of UiO-66 and -67 materials

To investigate why initial simulations of UiO-66 yielded lower predicted surface areas than we obtained experimentally, TGAs of each material synthesized were analyzed to determine what percent of the total mass was composed of by the ligand. The ligand mass percent was calculated for each MOF assuming the presence of 4, 5, and 6 ligands per formula unit. These values were then compared to the TGA results to determine how many ligands were present relative to each node. As observed in Figures S4 and S5, the TGAs of UiO-66 and UiO-67 show initial solvent loss near 75 °C followed by a drop at 300 °C which is attributed to the dehydration of the $Zr_6O_4(OH)_4$ nodes to Zr_6O_6. At this point the molecular formula of the framework is $Zr_6O_6L_x$ (L = bdc or bpdc, x = 1-6), depending on which framework was being analyzed and how many ligands are present. The final step near 500 °C is attributed to decomposition of the organic linkers. By calculating the percent of mass lost between these two plateaus and comparing to the expected mass loss for various numbers of ligands, we were able to estimate how many ligands were present. Table S2 compares the experimental mass loss shown in the TGAs with expected mass loss for frameworks containing 4, 5, and 6 ligands per formula unit for UiO-66 and -67. Attempts to analyze UiO-66-derivatives were not possible due to the thermal instability of the MOF (i.e., no clear plateau) over the desired temperature range. It should be noted that 4 linkers per formula unit is equivalent to 8 linkers coordinated to each node.

This journal is © The Royal Society of Chemistry 2013

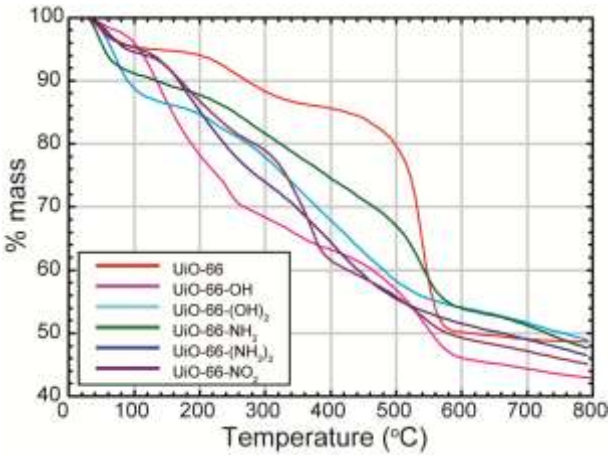

Figure S8. TGA plots of UiO-66 and functionalized derivatives.

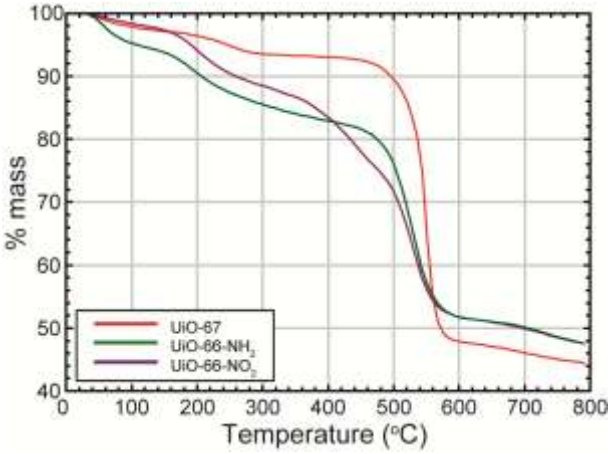

Figure S9. TGA plots of UiO-67 and functionalized derivatives.

Table S3. TGA analysis of UiO-66 and -67 used to determine the number of ligands present per formula unit in each.

	Experimental % Mass Loss	% Mass Loss 4 Ligands	% Mass Loss 5 Ligands	% Mass Loss 6 Ligands
UiO-66	43.3	43.1	49.5	54.6
UiO-67	52.3	53.9	59.9	64.5

Section S7. Simulated N_2 isotherms and geometric surface areas of UiO-66 structures

Grand canonical Monte Carlo (GCMC) simulations were performed to calculate N_2 isotherms at 77 K in UiO-66 and a modified UiO-66 structure containing only 4 linkers per formula unit. N_2 adsorption isotherms were calculated using a 2x2x2 unit cell. At each pressure, 40,000 total Monte Carlo cycles were performed, 20,000 to equilibrate the system and 20,000 to compute ensemble averages. In each cycle, an average of *N* moves was performed, where *N* is the number

of N_2 molecules in the system. Translation, rotation, insertion, deletion, and reinsertion moves were used. N_2 interactions with framework atoms were described using Lennard-Jones (LJ) potentials. Parameters for the framework atoms were taken from the DREIDING[9] force field and the Universal Force Field (UFF)[10] for those atoms not available on DREIDING. N_2 LJ parameters were taken from the TraPPE[11] model. Cross-terms were calculated using Lorentz Berthelot mixing rules. A cut off of 12.8 Å was used for all LJ interactions. N_2/N_2 interactions were described using a LJ + Coulomb potential, with the LJ parameters and charges taken from the TraPPE model. Charges of -0.482 are placed on the N nuclei and a +0.964 charge at the center of mass. Ewald sums were used for all Coulombic interactions. All calculations were performed using our in-house code RASPA.[12]

UiO-66 and UiO-67 structure analogues were generated by modifying the parent material with the corresponding functionalization and/or removal of linkers. Subsequently, the unit cell was geometrically optimized, modifying the parameters of the unit cell and the atomic coordinates. Bonded and short range interactions between the atoms were modeled using UFF parameters. A cut-off distance of 18.5 Å was used for the van der Waals interactions during the geometry optimization. These calculations were performed with the Forcite module of Materials Studio.[5]

Geometric surface areas of all the generated structures were calculated by rolling a 3.681 Å-diameter sphere, which corresponds to a nitrogen molecule, over the surface of the material.[13]

Figure S9 illustrates the comparison between simulation and experiment for N_2 adsorption at 77 K in UiO-66 with no linkers missing. Simulations and experiments agree reasonably well. However, we see deviations when comparing simulations with experiments in UiO-66 with only 4 linkers per formula unit, as illustrated in Figure S10. This could be due to multiple phenomena. When simulating this structure, a perfect crystal with 4 linkers per formula unit was used. However, experimentally, multiple crystals with various numbers of missing linkers may exist, with an overall average of 4 linkers present per formula unit.

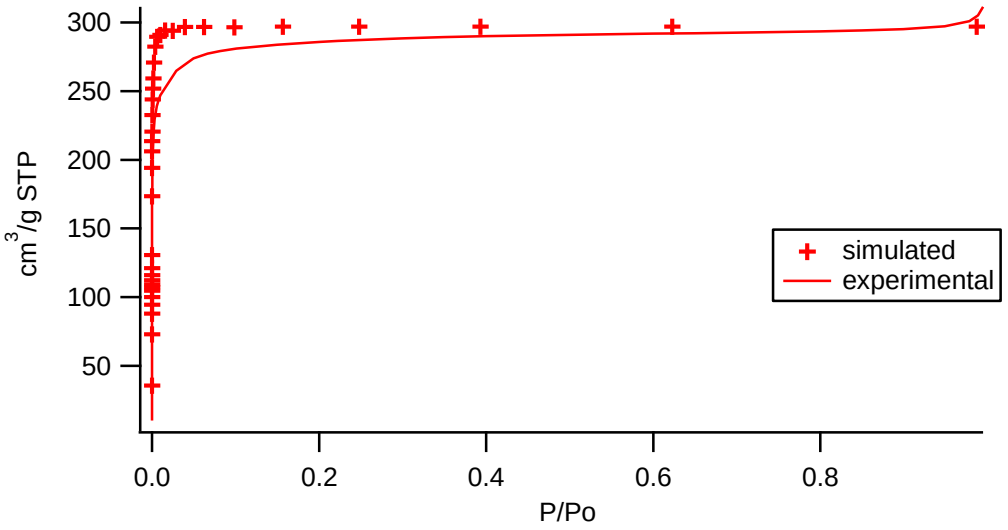

Figure S10. N_2 isotherms at 77K for UiO-66 without missing linkers.

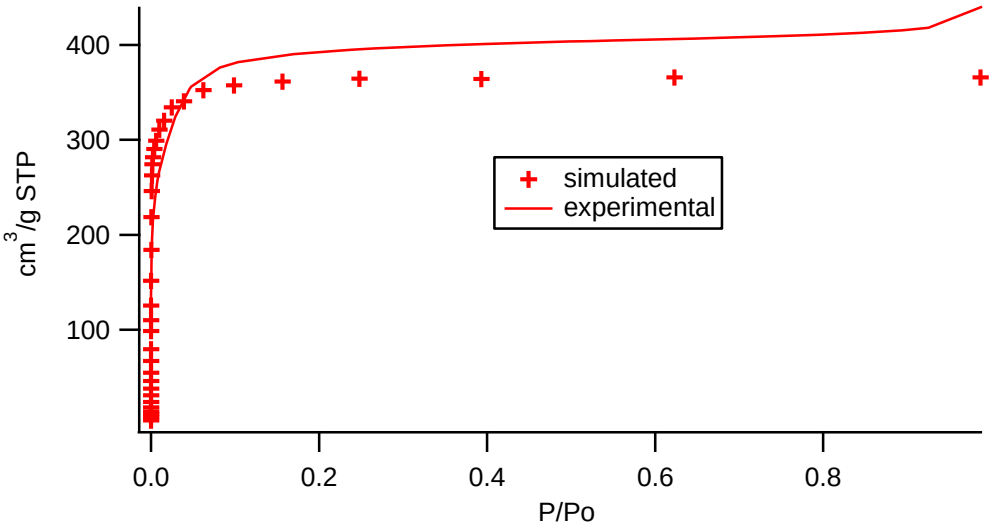

Figure S11. N_2 isotherms at 77K for UiO-66 with 4 linkers per formula unit.

The geometric surface area calculations assuming 4 linkers per formula unit (1550 m^2/g) agree very well with the experimental BET result (1580 m^2/g), as can be seen in Table 1. (As noted above, 4 linkers per formula unit is equivalent to each node coordinating 8 linkers). From the simulated isotherm for the structure with 4 linkers per formula unit, we calculated a BET surface area of 1400 m^2/g, but given the discrepancy between the isotherms, this difference is not unexpected. Similar agreement is observed in other functionalized versions of UiO-66 with and without missing linkers (Table 1).

Somewhat different results are obtained for UiO-67, where the geometric surface area calculated for the structure with no missing linkers (2700 m^2/g) agrees better with the experimental surface area (2500 m^2/g) than the geometric surface area for the structure with missing linkers (3100 m^2/g). See Table 1. This is somewhat surprising, given that TGA results suggest that UiO-67 also has only 4 linkers per formula unit. Incomplete activation of UiO-67 might explain these results.

This journal is © The Royal Society of Chemistry 2013

Section S8. IR spectra of UiO-66 synthesized conventionally[4] and with HCl

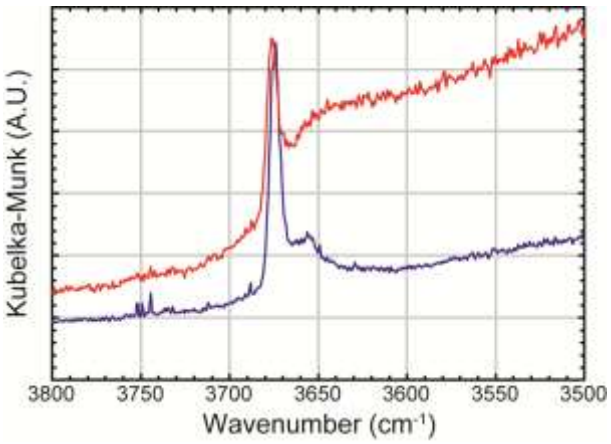

Figure S12. IR spectra of UiO-66 synthesized with missing linkers (blue) compared to UiO-66 synthesized via literature procedures with all of the expected linkers (red).

Section S9. Large-scale synthesis of UiO-66

In order to demonstrate the utility of our synthetic procedure, a large-scale synthesis of UiO-66 made with 4 grams of $ZrCl_4$ yielded 7.2 grams of pre-activated UiO-66. The surface area of this material was 1500 m^2/g. Although this large-scale procedure is compelling, we recognize that commercialization of UiO-66 would require a reactor capable of making kg quantities of UiO-66 with minimal use/loss of solvent.

Figure S13. Large scale synthesis of UiO-66 made via the HCl-containing procedure presented herein.

This journal is © The Royal Society of Chemistry 2013

Section S10. References

1. D. Himsl, D. Wallacher and M. Hartmann, *Angew. Chem. Int. Ed.*, 2009, **48**, 4639.
2. B. Vercelli, G. Zotti, A. Berlin, M. Pasini and M. Natali, *J. Mater. Chem.*, 2011, **21**, 8645.
3. R. K. Deshpande, J. L. Minnaar and S. G. Telfer, *Angew. Chem. Int. Ed.*, 2010, **49**, 4598.
4. A. Schaate, P. Roy, A. Godt, J. Lippke, F. Waltz, M. Wiebcke and P. Behrens, *Chem. Eur. J.*, 2011, **17**, 6643.
5. *Materials Studio*, Accelrys Software Inc., Sand Diego, CA 92121, USA.
6. P. M. Schoenecker, G. A. Belancik, B. E. Grabicka and K. S. Walton, *AlChE J.*, 2012, **59**, 1255.
7. O. G. Nik, X. Y. Chen and S. Kaliaguine, *J. Membr. Sci.*, 2012, **413-414**, 48.
8. C. Zlotea, D. Phanon, M. Mazaj, D. Heurtaux, V. Guillerm, C. Serre, P. Horcajada, T. Devic, E. Magnier, F. Cuevas, G. Férey, P. L. Llewellyn and M. Latroche, *Dalton Trans.*, 2011, **40**, 4879.
9. S. L. Mayo, B. D. Olafson and W. A. Goddard, *J. Phys. Chem.*, 1990, **94**, 8897.
10. A. K. Rappé, C. J. Casewit, K. S. Colwell, W. A. G. III and W. M. Skiff, *J. Am. Chem. Soc.*, 1992, **114**, 10024.
11. J. J. Potoff and J. I. Siepmann, *AlChE J.*, 2001, **47**, 1676.
12. D. Dubbeldam, S. Calero, D. E. Ellis and R. Q. Snurr, *RASPA*, (2008) Northwestern University, Evanston, IL.
13. T. Duren, Y.-S. Bae and R. Q. Snurr, *Chem. Soc. Rev.*, 2009, **38**, 1237.